Acta Mechanica Solida Sinica, Vol. 22, No. 3, June, 2009 ISSN 0894-9166
Published by AMSS Press, Wuhan, China

THEORETICAL MODEL OF EFFECTIVE STRESS COEFFICIENT FOR ROCK/SOIL-LIKE POROUS MATERIALS **

Kai Zhang Hui Zhou* Dawei Hu Yang Zhao Xiating Feng

(*State Key Laboratory of Geomechanics and Geotechnical Engineering, Institute of Rock and Soil Mechanics, Chinese Academy of Sciences, Wuhan* 430071*, China*)

Received 16 September 2008; revision received 8 January 2009

ABSTRACT Physical mechanisms and influencing factors on the effective stress coefficient for rock/soil-like porous materials are investigated, based on which equivalent connectivity index is proposed. The equivalent connectivity index, relying on the meso-scale structure of porous material and the property of liquid, denotes the connectivity of pores in Representative Element Area (REA). If the conductivity of the porous material is anisotropic, the equivalent connectivity index is a second order tensor. Based on the basic theories of continuous mechanics and tensor analysis, relationship between area porosity and volumetric porosity of porous materials is deduced. Then a generalized expression, describing the relation between effective stress coefficient tensor and equivalent connectivity tensor of pores, is proposed, and the expression can be applied to isotropic media and also to anisotropic materials. Furthermore, evolution of porosity and equivalent connectivity index of the pore are studied in the strain space, and the method to determine the corresponding functions in expressions above is proposed using genetic algorithm and genetic programming. Two applications show that the results obtained by the method in this paper perfectly agree with the test data. This paper provides an important theoretical support to the coupled hydro-mechanical research.

KEY WORDS rock/soil-like porous materials, generalized model for effective stress coefficient tensor, equivalent connectivity index of pore, genetic algorithm

I. INTRODUCTION

Based on the research on consolidation of saturated soil and the interaction between fluid and soil, Terzaghi[1] brought forward the effective stress law, which can be expressed as

$$\sigma_{ij}^e = \sigma_{ij}^t - \delta_{ij} p \tag{1}$$

where δ_{ij} is the Kronecker delta, σ_{ij}^e the effective stress tensor, σ_{ij}^t the total stress tensor and p the fluid pressure.

However, many experiments on the deformation of rock/soil-like porous materials under pore pressure have indicated that Terzaghi's effective stress law is not suitable for many materials. Then modified

* Corresponding author. Email: hzhou@whrsm.ac.cn

** Project supported by the Yalongjiang River Joint Fund by the National Natural Science Foundation of China (NSFC) and Ertan Hydropower Development Company, LTD (Nos. 50579091 and 50539090), NSFC (No. 10772190) and Major State Basic Research Project of China (No. 2002CB412708).

effective stress law was promoted[2]:

$$\sigma_{ij}^{e} = \sigma_{ij}^{t} - \delta_{ij}\alpha p \tag{2}$$

where α is the effective stress coefficient which ranges from 0 to 1. Based on experiment, Walsh[3] proved $\alpha = 0.9$ for the rockmass containing polishing joint, and Kranz[4] pointed out $\alpha = 0.56$ for the rockmass containing tensive joint.

The effective stress coefficient plays an important role in the coupled hydro-mechanical analysis because it denotes the influence of fluid pressure on the solid matrix of the porous media. Various equations for effective stress coefficient have been promoted[5], but none of them is widely used. Nur and Byerlee[6] proposed a theoretical model of effective stress coefficient with the assumption that the solid matrix is elastic media. Many researchers have studied the evolution law of effective stress coefficient with the deformation of the solid matrix based on the experiments and tried to find out the physical mechanism. Shao and Lu etc.[7–10] obtained the relation between strain and fluid pressure under different confined stress and deviatoric stress. Their results showed that the relation between the strain and the fluid pressure is nonlinear and the traditional effective stress law should be modified when the fluid pressure is high, and also with the fluid pressure increasing, the axial deformation of the rock sample decreases while the lateral deformation increases. This is to say, the deformation of rock due to the fluid pressure is obviously anisotropic. Bernabe[11], Sun[12,13] and Zhao[14] found that the effective stress coefficient is not a constant and varies with the effective confined stress and the fluid pressure. These results indicate that the effective stress coefficient has a close relation with the structure of pore. With the elastic assumption, Zhao[15] studied the effective stress law for coal samples under gas pressure, and the results showed that the effective stress coefficient varies bilinearly with the hydrostatic stress and the gas pressure. Feng etc.[16] studied the relation between the volumetric stress and the fluid pressure to the effective stress coefficient using numerical method and the results are consistent with Ref.[15].

The effective stress coefficient is influenced by the microstructure of the pore and fissure, the deformation of solid matrix and the stress conditions, so it is very difficult to obtain a strict theoretical model for the coefficient. The former studies were mostly focused on special porous materials, and aimed to obtain experiential equations of effective stress coefficient based on the test data. Although the results are useful for those special porous materials, they are not applicable for other porous media. In order to establish a generalized model for the effective stress coefficient, the physics mechanism of fluid-solid interaction should be thoroughly analyzed.

The purpose of this paper is to bring forward a generalized theoretical model to study the effective stress coefficient for rock/soil-like porous materials based on the basic theories of continuous mechanics and tensor analysis. Then the case studies will be conducted to examine the validity of the model.

II. EFFECTIVE STRESS COEFFICIENT

2.1. Some Factors Influencing on Effective Stress Coefficient and Physical Mechanism

The effective stress is averagely generalized to be an equivalent of the contact force among grains in unit area[17]. The effective stress coefficient, in a cross section in the porous material, denotes the ratio of the area occupied by the fluid to the total area[18]. For the granular soil (as shown in Fig.1), the contact area among grains is very small, so any cross section can be replaced by a curved face, which is almost occupied by the fluid. Therefore the corresponding effective stress coefficient α approximately equals to 1. However, for rock/soil-like porous materials composed of crystallization or cementation as shown in Fig.2, the curved face, similar to that in Fig.1, does not exist, so the effective stress coefficient α is less than 1. The pore structure of porous materials composed of crystallization or cementation is shown in Fig.2, and Fig.2(b) is the Representative Element Area (REA) in an arbitrary cross section in Fig.2(a). Here the normal unit vector of the section is i.

In Fig.2(b), let A_i denote the area of REA, A_{vi} and A_{si} denote respectively the area of the pore and the solid in REA, then:

$$n_{Ai} = \frac{A_{vi}}{A_i} \tag{3}$$

where n_{Ai} is the area porosity of REA.

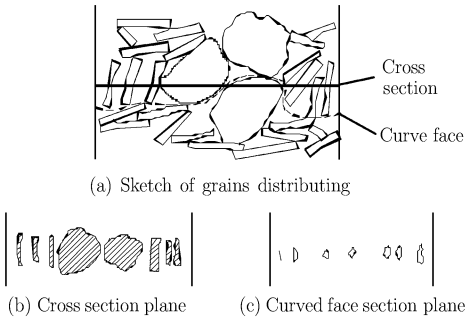

Fig. 1. Sketch of the effective stress coefficient $\alpha = 1$ for soil and soil-like materials[19].

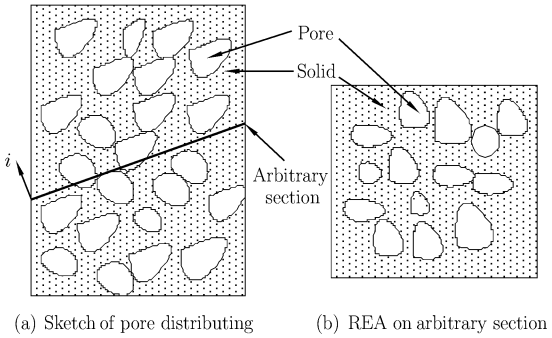

Fig. 2. Sketch of pore structure in the rock or soil composed of crystallization or cementation.

When the porous material is saturated, pores in the area A_{vi}, as well as the initial cracks and the cracks induced by deformation in the solid matrix, are full of fluid. Here let $(A_{si})_p$ denote the area of the cracks in A_{si}, which is full of fluid (not presented in Fig.2), then we can define a parameter γ_i, called equivalent connectivity index in this study, as the following:

$$\gamma_i = \frac{(A_{si})_p}{A_{si}} \quad (0 \leq \gamma_i \leq 1) \tag{4}$$

From Eq.(4), we can find that γ_i represents the connectivity of pores in the REA, and depends on the structure of cracks and pores and the property of the fluid in them.

For the REA as shown in Fig.2(b), let $\boldsymbol{\sigma}^t$ and $\boldsymbol{\sigma}^e$ denote respectively the total stress tensor and the effective stress tensor, based on the definition of effective stress and the force equilibrium on the area, then we can obtain the equation below on an average sense.

$$(\boldsymbol{\sigma}^e \cdot \boldsymbol{i})A_i = (\boldsymbol{\sigma}^t \cdot \boldsymbol{i})A_i - (\boldsymbol{I} \cdot \boldsymbol{i})(A_{vi} + \gamma_i A_{si})p \tag{5}$$

where $\boldsymbol{i}$ is the normal unit vector of the REA, p is the fluid pressure, and $\boldsymbol{I}$ is the unit tensor.

Because $A_{si} = A_i - A_{vi}$, Eq.(5) can be rewritten from Eq.(4) as

$$\boldsymbol{\sigma}^e = \boldsymbol{\sigma}^t - [n_{Ai} + (1 - n_{Ai})\gamma_i]\, p \cdot \boldsymbol{I} \tag{6}$$

By comparing Eq.(6) with Eq.(2), we can obtain:

$$\alpha_i = n_{Ai} + (1 - n_{Ai})\gamma_i \tag{7}$$

where α_i is the effective stress coefficient of the REA.

In Fig.2(a), let V and V_v denote the volume of the total porous material and the volume of pores, respectively, and n denote the volumetric porosity, then:

$$n = \frac{V_v}{V} \tag{8}$$

In the porous material as shown in Fig.2(a), select a column Representative Element Volume (REV) with the height of L and the axis s parallel to $\boldsymbol{i}$, then the volume of the REV is

$$V' = \int_L A \mathrm{d}s \tag{9}$$

where A is the area of the cross section of the column.

Let n_i be the volumetric porosity of the REV, then we can obtain:

$$n_i V' = \int_L n_{Ai}(s) \cdot A \mathrm{d}s \tag{10}$$

where $n_{Ai}(s)$ is the area porosity of the cross section along the axis s. As $n_{Ai}(s)$ is independence of A, Eq.(10) can be rewritten as

$$n_i V' = A \cdot \int_L n_{Ai}(s)\mathrm{d}s \tag{11}$$

In the REV, we define $\bar{n}_{Ai}$ as the average area porosity of all cross sections perpendicular to the axis s, then:

$$\bar{n}_{Ai} = \frac{1}{L}\int_L n_{Ai}(s)\mathrm{d}s \tag{12}$$

As $V' = A \cdot L$, we can obtain from Eqs.(11) and (12):

$$n_i = \bar{n}_{Ai} \tag{13}$$

Obviously, the volumetric porosity of the column equals to the average area porosity of the cross section normal to the axis of the column.

If the rock/soil-like porous materials are homogeneous, we obtain:

$$n_i = n, \qquad n_{Ai} = \bar{n}_{Ai} \tag{14}$$

From Eqs.(13) and (14), the following equation can be obtained:

$$n_{Ai} = n \tag{15}$$

Using Eqs.(15) and (7), the equation for the effective stress coefficient can be expressed as

$$\alpha_i = n + (1-n)\gamma_i \tag{16}$$

If the porous material is anisotropic, the effective stress coefficient and equivalent connectivity index are both second-order tensor. Let $\boldsymbol{\alpha}$ and $\boldsymbol{\gamma}$ denote respectively the stress coefficient tensor and equivalent connectivity index tensors, then:

$$\boldsymbol{\alpha} = n\boldsymbol{I} + (1-n)\boldsymbol{\gamma} \tag{17}$$

If the porous material is isotropic, $\boldsymbol{\alpha} = \alpha\boldsymbol{I}$ and $\boldsymbol{\gamma} = \gamma\boldsymbol{I}$, where α and γ are scalars, and $\boldsymbol{I}$ is the unit second-order tensor. Then Eq.(17) can be simplified as

$$\alpha = n + (1-n)\gamma \tag{18}$$

From the analysis above, we can find that effective stress coefficient is the inherent property of both the porous material and the fluid in the pores, and depends on the microstructure of pores or the fissure and the property of the fluid.

Because the macroscopic deformation can reflect the microstructure of porous material directly, we discuss the evolution of porosity and equivalent connectivity index in the strain space. Due to the difficulty of the problem, present research only focuses on the material undergoing elastic deformation and does not consider the influence of the property difference of the fluid.

2.2. Evolution of Parameters in Strain Space

Some rock/soil-like porous materials, such as marble and granite, are composed of crystallization or cementation. According to the measured permeability and the character of pores, the porosity here is defined to be high when the porosity is between 5% and 40%, and the porosity is defined to be low when the porosity is less than 5%. If the porosity is low, the main factor influencing the effective stress coefficient is the equivalent connectivity index and the porosity can be considered to be invariable during the deformation under the elastic condition. If the porosity is high, the grain can be assumed to be incompressible with the consideration that the compressibility of the grain is very small comparing with that of the skeleton. Under the elastic condition, the deformation of the material is caused by the rearrangement of the pore structure. If the material is considered to be equivalent continuum, the volume of cracks and its variety can be neglected although there are new stress-induced cracks during the deformation. But cracks change the connectivity of the pore and influence the equivalent connectivity index.

For the porous materials with high porosity as defined above, the grain can be assumed to be incompressible and the volume of cracks and its variety can be neglected. Then letting the compressive stress be positive, we obtain:

$$V = V_0(1 - \varepsilon_v), \qquad V(1 - n) = V_0(1 - n_0) \tag{19}$$

where V_0 and n_0 are the volume and porosity of the material before deformation, respectively; V and n are the volume and porosity of the material after deformation, respectively.

Then we obtain evolution of porosity n:

$$n = \frac{n_0 - \varepsilon_v}{1 - \varepsilon_v} \tag{20}$$

From the definition of equivalent connectivity index γ, we can find that γ mainly depends on the size and distribution of pores and microcracks and can be generally expressed as:

$$\gamma = f(\gamma_0, \varepsilon) \tag{21}$$

where γ_0 is the initial equivalent connectivity index, and ε is a strain parameter of the porous material and here we define it as the volumetric strain for isotropic and elastic materials.

Then, we can use the Eqs.(18), (20) and (21) to study the evolution of effective stress coefficient, and summarize them as

$$n = \frac{n_0 - \varepsilon_v}{1 - \varepsilon_v}, \quad \gamma = f(\gamma_0, \varepsilon), \quad \alpha = n + (1 - n)\gamma \tag{22}$$

However, due to the complexity of the micro-structure of rock/soil-like material and its evolution induced by stresses, it is impossible to obtain a theoretical form for equivalent connectivity index γ in the strain space. The function f in Eq.(22) can be determined using the method below.

2.3. Identifying Structure and Parameters of Function Using Genetic Programming and Genetic Algorithm

An intelligent method is introduced to determine the form of the function f in Eq.(22). We only give a simple introduction for this method in the following paragraphs, and the detailed can be referred to Ref.[20].

Genetic algorithm (GA) is an optimizing method to simulate biology evolving processes. The algorithm applies the Darwinian principle of natural selection ('survival of the fittest') to a set of tentative solutions, generally coded in binary or real number strings, of the discussed solution. It is one of the random search algorithms. It has a fast search function in the optimum space and a strong ability of error tolerance. It is attractive to the problem that is without or with few heuristic solutions. A fitness function is used to evaluate the fitness of the tentative solution. Some genetic operations such as reproduction, crossover, and mutation, etc. are performed on the old tentative solutions , for creating a set of new tentative solutions. The fitness function is used again to evaluate the applicability of the new tentative solution. The evolving process does not finish until the fittest solution is found.

Genetic programming (GP) is a new structure description method. Its nature is a generalized hierarchy computer program description. It does not need to determine in advance or restrict the form of the structure and its size. The description can automatically modify the size of the structure according to its environment change. Therefore, it is attractive in the recognition of the structure of non-linear constitutive material model.

By coupling the GA and GP, we can identify the structure and parameters of the function f simultaneously, and the procedure is shown in Fig.3.

III. CASE STUDIES

3.1. Effective Stress Coefficient of Coal under Elastic and Isotropic Condition

In Ref.[15], Zhao etc. studied the deformation of coal under gas pressure by experiments. The preconditions of the experiment are: (1) the coal is homogeneous and isotropic; (2) the deformation of the coal matrix is elastic and reversible. Although these assumptions do not perfectly fit the material,

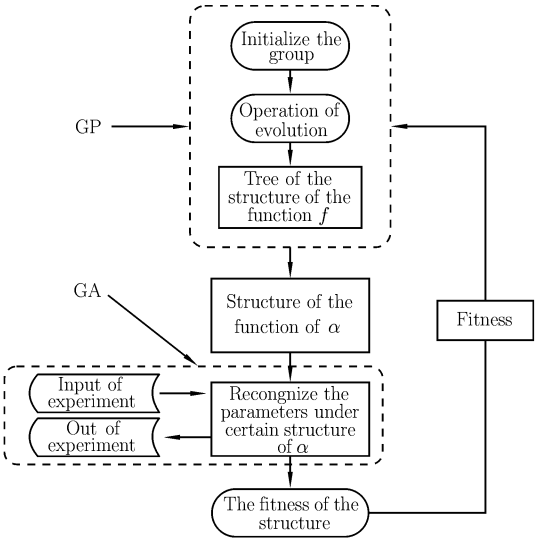

Fig. 3. Procedure to identify the structure and parameters of the function f.

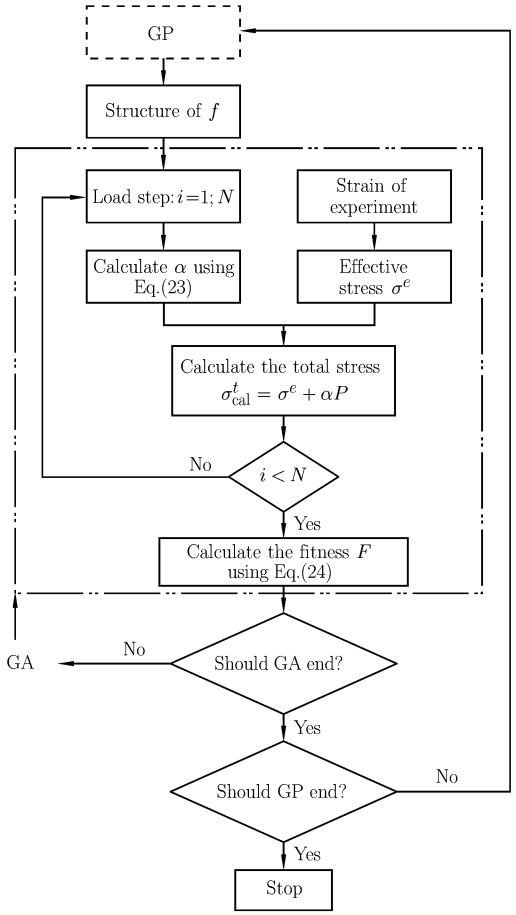

Fig. 4. Procedure to identify the function f.

the authors argued that they have good approximation. According to the experiment, the initial porosity is 6.07%, Young's modulus is 2.174 GPa and Poisson's ratio is 0.313.

Under the assumption of isotropy and elasticity, the volumetric strain ε_v can represent the deformation of the coal, and is selected as an internal variable in this study. If ε_v is the volumetric strain induced by exterior force and $\delta\varepsilon_v$ is the volumetric strain caused by the fluid pressure, we obtain $\varepsilon_v \geq 0$, $\delta\varepsilon_v \leq 0$ and the total volumetric strain is $\varepsilon_v + \delta\varepsilon_v$. Then according to Eq.(22), we have

$$n = \frac{n_0 - (\varepsilon_v + \delta\varepsilon_v)}{1 - (\varepsilon_v + \delta\varepsilon_v)}, \quad \gamma = f\left(\gamma_0, \varepsilon_v, \delta\varepsilon_v\right), \quad \alpha = n + (1-n)\,\gamma \tag{23}$$

The structure and parameters of function f in Eq.(23) can be identified using the method described in §2.3, and details are shown in Fig.4. In order to validate the method proposed in this study, we divide the experimental data into two groups, one group is used to determine the structure and parameters of the function$f$ in Eq.(23), and the other group is used to verify the results. The second group includes the data with hydrostatic pressure of 8MPa, and the other data belongs to the first group. In order to simplify the structure of the function f, only two operators, add and multiply, are set in the structure, and the maximum depth of the tree of the structure is 5. Both GA and GP terminate when the number of iteration reaches 10. The evo-

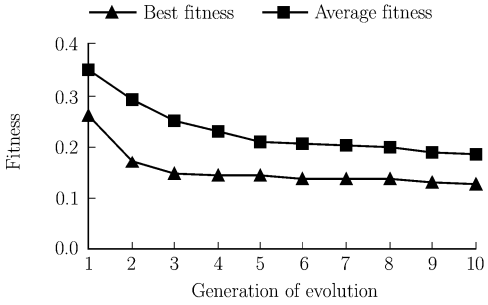

Fig. 5 Evolution of the best and average fitness.

lutions of the best fitness and the average fitness are shown in Fig.5, from which we can find that the structure of the function f is improved step by step.

$$F = \sqrt{\frac{\sum_{i=1}^{N} \left(\sigma_{\text{cal}}^{t} - \sigma^{t}\right)^{2}}{N}} \tag{24}$$

where N is the total load steps, σ^t and σ_{cal}^t are the total stresses of experiment and calculation, respectively.

The structure with the best fitness is:

$$f_1 = \gamma_0 + c_1\varepsilon_v + c_2\delta\varepsilon_v \tag{25}$$

where γ_0, c_1 and c_2 are parameters and depend on the size and distribution of pores and the property of the gas. Here, the values of the parameters are: $\gamma_0 = 0.60$, $c_1 = -120.5$ and $c_2 = -351.2$. We can find that the function f (equivalent connectivity index) is more sensitive to $\delta\varepsilon_v$, i.e., it is more sensitive to the fluid pressure than the exterior force.

From Eqs.(23) and (25), the strain at different hydrostatic stress and fluid pressure can be deduced, and then the effective stress coefficient can be calculated. Therefore, the change of the strain of the coal under the gas pressure can be estimated using Eq.(26), and the estimated results, together with experiment results, are shown in Fig.6. We can find that the estimated results perfectly agree with the experimental data.

$$\delta\varepsilon_1 = \delta\varepsilon_2 = \delta\varepsilon_3 = \frac{-(1-2\mu)}{E}\alpha p \tag{26}$$

From Fig.6, we can find out that when the hydrostatic pressure increases, the strain induced by the constant fluid pressure decreases. Under the same hydrostatic stress, the strain increases nonlinearly

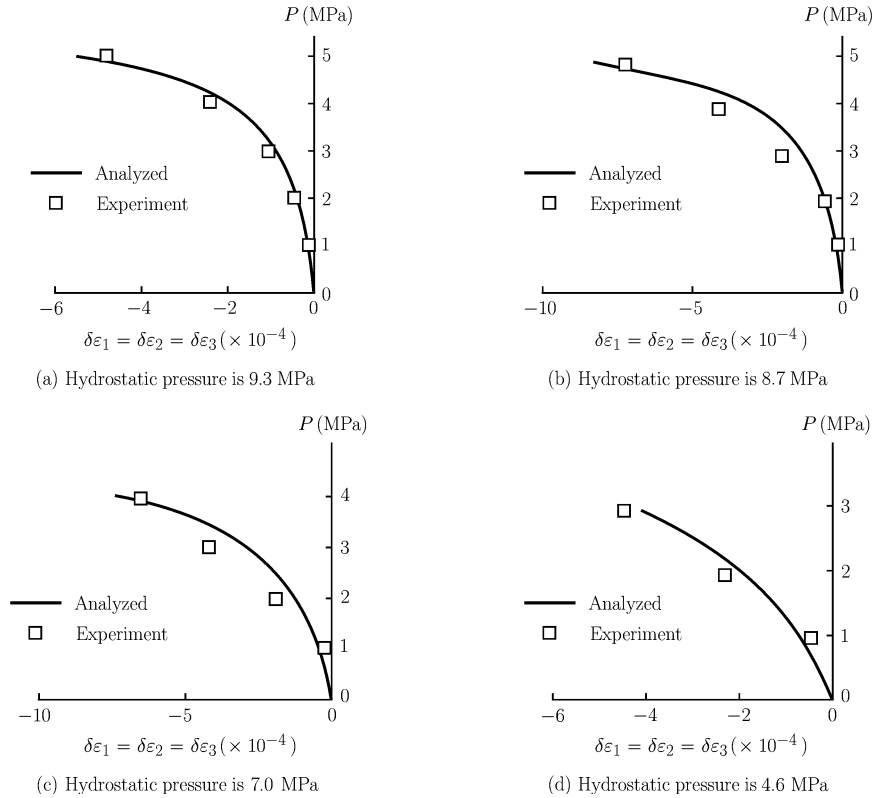

Fig. 6. Relationship between strain increment and fluid pressure under different hydrostatic stress.

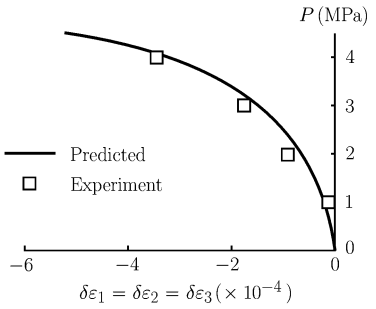

Fig. 7. Relationship between strain increment and fluid pressure under hydrostatic stress of 8 MPa.

with the fluid pressure. The same method above is used to predict the response of the coal to the gas pressure under 8 MPa hydrostatic stress, and the result is shown in Fig.7. We can find that the experiment and predicted results are also consistent.

3.2. Effective Stress Coefficient of Sandstone under Elastic and Anisotropic Condition

In Ref.[21], Lu experimentally studied the mechanical property and effective stress of the sandstone based on experiments. These experiments are performed under four confining pressures: 10 MPa, 20 MPa, 30 MPa and 40 MPa. We here just list the results under the confining pressure of 40 MPa in Figs.8 and 9 in which P_w is the pore pressure. We can find that when the deviatoric stress $(\sigma_1 - \sigma_3)$ is less than 100 MPa, the deformation of the sandstone is elastic and the relation between the strain and the fluid pressure is linear. But when the fluid pressure increases, the first principle strain ε_1 and the third principle strain ε_3 decrease with different rate, that is to say, the deformation of the sandstone under fluid pressure is anisotropic. Then, the effective stress coefficient and the equivalent connectivity index are both second-order tensors. Considering the symmetry, two of the three principal components of effective stress coefficient tensor and the equivalent connectivity index tensor are equal to each other.

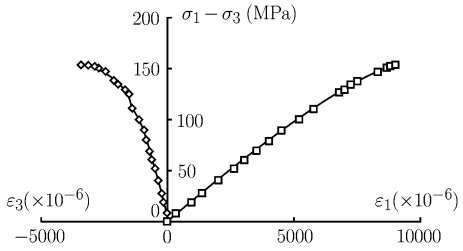

Fig. 8. Experimental data of sandstone with the confining stress of 40 MPa.

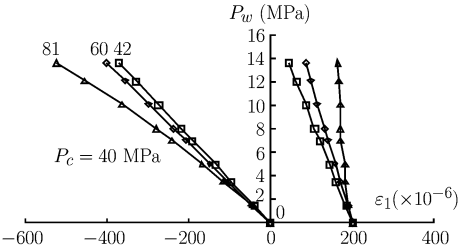

Fig. 9. Experimental strain responses to pore pressure change under the deviatoric stress (indicated by the numbers) with the confining stress of 40 MPa.

From Eq.(17), the unit principle axis vector of the effective stress coefficient tensor and the equivalent connectivity index tensor are the same. Assuming that the principle axes of effective stress coefficient tensor correspondingly coincide with those of the strain, similarly to the discussion for the isotropy in §2.2, the effective stress coefficient tensor can be expressed as

$$n = \frac{n_0 - \varepsilon_v}{1 - \varepsilon_v}, \quad \boldsymbol{\gamma} = f(\boldsymbol{\varepsilon}), \quad \boldsymbol{\alpha} = n\boldsymbol{I} + (1-n)\boldsymbol{\gamma} \tag{27}$$

where n_0 is the initial porosity and equals to 19%, $\boldsymbol{\gamma}$ the equivalent connectivity index tensor and $\boldsymbol{I}$ the second-order unit tensor.

Then the last two equations in Eq.(27) can be expressed by principle values:

$$\gamma_1 = f(\varepsilon_1), \quad \gamma_2 = f(\varepsilon_2), \quad \alpha_1 = n + (1-n)\gamma_1, \quad \alpha_2 = n + (1-n)\gamma_2 \tag{28}$$

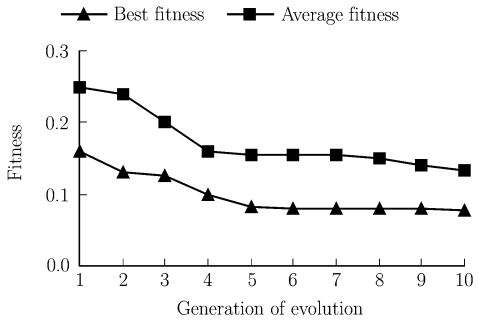

Fig. 10. Evolution of the best and average fitness.

where γ_1 and γ_2 are the principle values of tensor $\boldsymbol{\gamma}$, α_1 and α_2 are the principle values of tensor $\boldsymbol{\alpha}$.

In order to validate the method proposed in this paper, we also divide the experimental data into two groups, one group is used to determine the structure and parameters of the function$f$ in Eq.(28), and the other group is used to verify the results. The second group includes the data under the confining stress of 20MPa, deviatoric stress $(\sigma_1 - \sigma_3) = 50$ MPa and the confining stress of 40 MPa, deviatoric stress $(\sigma_1 - \sigma_3) = 81$ MPa. And the other data belong to the first group. The structure and parameters of the function f in Eq.(28) are identified using the method stated in §3.1. The number of operators in the structure is restricted to 4, i.e., add, multiply, natural logarithm and exponent. The maximum depth of the tree is restricted to 4. Both GA and GP terminate when the number of iteration reaches 10. The evolution of the best fitness and average fitness are shown in Fig.10, from which we can find that the structure of the function f is improved step by step.

The structure of f with the best fitness and simplest form is:

$$f = c_1 \ln(\boldsymbol{\varepsilon}) + c_2 \tag{29}$$

where c_1 and c_2 are parameters and depend on the size and the distribution of the grains and the property of the fluid. Here, the value of parameters are: $c_1 = -0.278$ and $c_2 = -1.33$. As $0 \leq \gamma_i \leq 1$ $(i = 1, 2)$, when $\varepsilon_i \leq 2.3 \times 10^{-4}$, $\gamma_i = 1$. That is to say, before the sandstone is loaded, the principle value of equivalent connectivity index tensor is 1. Then, at the initial state, Terzaghi's effective stress law can be used for the sandstone.

From Eqs.(28) and (29), the effective stress coefficient tensor at different strain state can be deduced. Then the change of the strain of the sandstone under fluid pressure can be estimated using Eq.(30). The data in the second group is used to check the method (as shown in Fig.11). The analyzed results perfectly agree with the test data.

$$\delta\varepsilon_1 = -(\alpha_1 - 2\mu\alpha_2)\frac{\delta P}{E}, \quad \delta\varepsilon_3 = -(\alpha_2 - \mu\alpha_2 - \mu\alpha_1)\frac{\delta P}{E} \tag{30}$$

where α_1 and α_2 are the principle values of tensor $\boldsymbol{\alpha}$, E and μ are Young's modulus and Poisson's ratio, respectively.

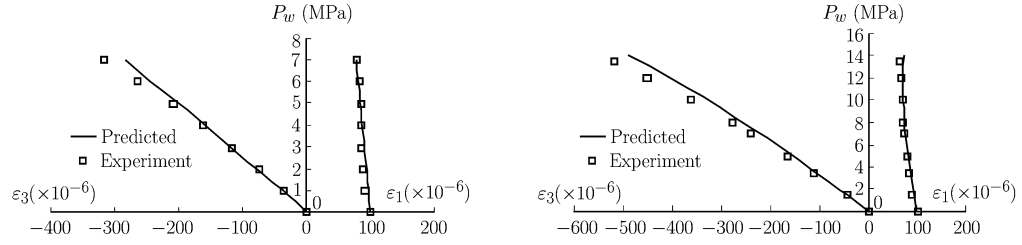

(a) Confining stress of 20 MPa and $\sigma_1 - \sigma_3 = 50$ MPa (b) Confining stress of 40 MPa and $\sigma_1 - \sigma_3 = 81$ MPa

Fig. 11. Strain responses to pore pressure (P_w) change under different confining stress and deviatoric stress.

IV. CONCLUSIONS

The effective stress law is studied based on achievements of the former researchers. A generalized method is proposed to analyze the effective stress coefficient for rock/soil like materials based on basic theories of continuous mechanics and the tensor analysis. Using the equivalent connectivity index, a generalized model is set up for effective stress coefficient tensor as shown in Eq.(17).

The effective stress coefficient model is simplified under the elastic and isotropic conditions. In the strain space, the evolution of porosity and equivalent connectivity index is investigated, then a method coupling GA and GP is proposed to identify the structure and parameters of the function, which is used to calculate the equivalent connectivity index.

In order to validate the method proposed, the deformation of the coal and the sandstone induced by the fluid pressure are studied. The results show that the present method can be used both for isotropic and anisotropic materials.

Acknowledgements The authors are grateful to Doctor Yang,C.X. and Doctor Chen,B.R. for their help in the program of GA and GP.

References

[1] Terzaghi,K.V., Die Berechnung der durchassigkeitsziffer des Tones aus dem Verlauf der hydrodynamischen Spannungserscheinungen. *Sitzungsber.Akad.Wiss.Wien Math Naturwiss*, 1923, 132(2A): 105-126.
[2] Biot,M.A., General theory of three-dimensional consolidation. *Journal of Application Physics*, 1941, 12: 155-160.
[3] Walsh,J.B., Effect of pore pressure and confining pressure on fracture permeability. *International Journal of Rock Mechanics and Mining Sciences & Geomechanic Abstract*, 1981, 18(3): 429-435.
[4] Kranz,R.L., Frankel,A.D., Engelder,T. and Scholz,C.H., The permeability of whole and jointed barre granite. *International Journal of Rock Mechanics and Mining Sciences & Geomechanics Abstracts*, 1979, 16: 225-234.
[5] Lade,P.V. and Boer,R.D., The concept of effective stress for soil, concrete and rock. *Geotechnique*, 1997, 47(1): 61-78.
[6] Nur,A. and Byerlee,J.D., An Exact Effective Stress Law for Elastic Deformation of Rock with Fluids. *Journal of Geophysical Research*, 1971, 76(26): 6414-6419.
[7] Shao,J.F., Poroelastic behaviour of brittle rock materials with anisotropic damage. *Mechanics of Materials*, 1998, 30(1): 41-53.
[8] Shao,J.F., Lu,Y.F. and Lydzba,D., Damage modeling of saturated rocks in drained and undrained conditions. *Journal of Engineering Mechanics*, *ASCE*, 2004, 130(6): 733-740.
[9] Karami,H., Experimental Investigation of Poroelastic Behaviour of a Brittle Rock. 1998, University of Lille I: Lille.
[10] Bart,M., Shao,J.F. and Lydzba,D., Coupled hydromechanical modeling of rock fractures under normal stress. *Canadian Geotechnical Journal*, 2004, 41(4): 686-697.
[11] Bernabe,Y., The effective pressure law for permeability in Chelmsford granite and Barre granite. *International Journal of Rock Mechanics and Mining Sciences*, 1986, 3(3): 267-275.
[12] Sun,P.D., Sun Model and Its Application. Hangzhou: Zhejiang University Press, 2002 (in Chinese).
[13] Sun,P.D., Xian,X.F. and Qian, Y.M., Experiment study on the effective stress in coal. *Mining Safety & Environmental Protection*, 1999, 2: 16-19 (in Chinese).
[14] Zhao,Y.S., Hydromechanics in Coal Rock. Beijing: China Coal Industry Publishing House, 1993 (in Chinese).
[15] Zhao,Y.S. and Hu,Y.Q., Experimental study of the law of effective stress by methane pressure. *Chinese Journal of Geotechnical Engineering*, 1995, 17(3): 26-31 (in Chinese).
[16] Feng,Z.C., Wu,H. and Zhao,Y.S., The numerical study of effective stresses law of rock mass. *Journal of TaiYuan University of Technology*, 2003, 34(6): 713-715 (in Chinese).
[17] Zhang,Y.T., Rock Hydraulics and Engineering. Beijing: China Waterpub Press, 2005 (in Chinese).
[18] Bear,J., Dynamics of fluids in Porous Media. New York: American Elsevier Publishing Company, 1972.
[19] Qian,J.H. and Yin,Z.Z., Geotechnique Principle and Computing. BeiJing: China Water Power Press, 1996 (in Chinese).
[20] Yang,C.X., Evolutionary Identification of Nonlinear Material model. ShenYang: Northeastern University, 2001 (in Chinese).
[21] Lu,Y.F., Modelisation de l'endommagement anisotrope des roches saturees in laboratoire de mecanique de lille. University des Sciences et Technologies de Lille, 2002.